

# Non linear electromechanical cart characterization using minimal modeling approach\*

N. Wongvanich<sup>1</sup>, C. E. Hann<sup>1</sup>, H. R. Sirisena<sup>1</sup>

**Abstract**—This paper presents a minimal modelling methodology for capturing highly non-linear dynamics in an electromechanical cart system. The second order differential equation model describing the cart system is reformulated in terms of integrals to enable a fast method for identification of both constant and time varying parameters. The model is identified based on a single experimental proportional step response and is validated on a proportional-derivative (PD) controlled step input for a range of gains. Two models with constant damping and time varying non-linear damping were considered. The fitting accuracy for each model was tested on three separate data sets corresponding to three proportional gains. The three data sets gave similar non-linear damping models and in all cases the non-linear model gave smaller fitting errors than the linear model. For the PD control responses, the constant damping model gave a higher average percentage prediction errors than the non-linear model. The non-linear model also provided significantly better PD control design. These results demonstrate the ability of the proposed method to accurately capture significant non-linearities in the data.

## I. INTRODUCTION

Many systems have non-linear oscillatory behaviour. Notable examples include building response to seismic load [1] and robotic arm [2]. Typical approach to analyzing vibration responses in various applications is to assume linear damping and break the responses into various modal frequencies. For example, modal analysis is commonly used for assessing damage of a building after an earthquake [3]. Another common approach is Prony's Analysis [4]. Other methods have involved non-linear regression analysis [5], and statistical methods such as the Mean-Likelihood estimator [6].

In electro-mechanical systems, significant non-linear damping exists, including static friction and gear backlash [7]. The usual approach to capturing this phenomena is to have a pre-assumed non-linear representation, for example, the Bingham viscoplastic model [8], and the Bouc-Wen model [9]. There are also several models of gear backlash [10]. Thus, the concept is to start with complex model structures first, and then fit it to the data. If required, more complex models of damping can be used including finite elements [11].

This work presents a different philosophy by starting with initially simplified structures for the model then using correlations between the time varying parameters and measured data to “bootstrap” a more complex and accurate non-linear

model [13]. It also allows an integral based method for parameter identification to be developed that transforms a non-linear and possibly non-convex optimization problem into a linear optimization. This identification method has been validated in first order systems, for example, biomedical applications [12], and rocket roll dynamics [14]. This paper extends the method to handle non-linear second order systems. Although, the focus of this paper is on the non-linear characterization and comparison with linear models; this extended integral method is important for minimizing computational requirements for the non-linear identification. The method is validated on an experimental electromechanical cart system with significant non-linear damping present. A second order non-linear model is identified on a single closed-loop response and is shown to accurately capture the system non-linear dynamics over a wide range of inputs. The non-linear model is shown to be significantly more accurate than a model with linear damping, but most importantly provides better control system prediction and design.

## II. METHODOLOGY

*A. Problem statement: linear spring with time-varying damping*

The normalized differential equation for a free vibrating linear spring is defined:

$$\ddot{y} + c\dot{y} + ky = 0 \quad (1)$$

$$\text{initial conditions} \equiv y(0) = y_0, \quad y'(0) = dy_0 \quad (2)$$

where  $y \equiv y(t)$  is the displacement (m),  $c$  the damping factor ( $kg/s$ ), and  $k$  the stiffness of the spring ( $N/m$ ).

Equations (1) and (2) describe the transient response of a spring-mass-damper which is useful for modelling the dynamics of single degree of freedom systems, including electro-mechanical systems [7]. In practice, the damping  $c$  in Equation (1) is often non-linear and can include dynamics of both static and dynamic friction and gear backlash [7], [8], [10]. The approach presented in this paper is to treat the damping  $c$  initially as time-varying then relating it to measured quantities like velocity and displacement. In other words, a simplified model is used to bootstrap more complex models to capture the measured response.

To allow flexibility in the model, a constant piecewise model of damping is used. Hence, Equation (1) is rewritten in the form:

$$\ddot{y} + c(t)\dot{y} + ky = 0 \quad (3)$$

\*This work was not supported by any organization

<sup>1</sup>N. Wongvanich, C. E. Hann, H.R. Sirisena are with the Department of Electrical and Computer Engineering, University of Canterbury, Christchurch, New Zealand. wongvanich@ieee.org

where:

$$\begin{aligned} c(t) &= c_1, \quad T_0 < t < T_1 \\ &= \vdots \\ &= c_n \quad T_{n-1} < t < T_{end} \end{aligned} \quad (4)$$

$$T_{i+1} - T_i = \Delta t, \quad i = 0, \dots, n-1 \quad (5)$$

$$\begin{aligned} T_0 &= 0, \quad \Delta t \equiv \text{user defined time interval,} \\ n &= \text{number of damping values} \end{aligned} \quad (6)$$

### B. Integral Method — time varying damping

To identify  $\{c_i, i = 1, \dots, n\}$  and  $k$  in Equations (3) and (4), an integral based approach is used. Equation (3) is first double integrated over time from  $T_{i-1}$  to  $t \in [T_{i-1}, T_i]$ , which yields:

$$\begin{aligned} y(t) - y_{i-1} - \alpha_{i-1}(t - T_{i-1}) + c_i \int_{T_{i-1}}^t y_m dt \\ + k \int_{T_{i-1}}^t \int_{T_{i-1}}^t y_m dt dt = 0 \end{aligned} \quad (7)$$

where:

$$y_{i-1} = y(T_{i-1}), \quad y'_{i-1} = y'(T_{i-1}), \quad i = 1, \dots, n \quad (8)$$

$$\alpha_{i-1} = y'_{i-1} + c_i y_{i-1} \quad (9)$$

The initial conditions of Equation (8) are defined at the beginning of each interval that the time-varying damping of Equation (4) is defined over. Let  $y_m(t)$  denote measured data in the system described by Equations (3) and (4). Define the function:

$$\begin{aligned} y_{\text{model},i}(t) &= y_{i-1} + \alpha_{i-1}(t - T_{i-1}) - c_i \int_{T_{i-1}}^t y_m dt \\ &- k \int_{T_{i-1}}^t \int_{T_{i-1}}^t y_m dt dt, \quad i = 1, \dots, n, \quad t \in [T_{i-1}, T_i] \end{aligned} \quad (10)$$

The initial conditions in Equation (10) are initially considered as unknown parameters and may not necessarily correspond to measured data points. For arbitrary values of these conditions, the function in Equation (10) could be discontinuous. To enforce  $C^1$  continuity, the following equality constraints are defined:

$$y_{\text{model},i}(T_i^-) = y_i, \quad y'_{\text{model},i}(T_i^-) = y'_i, \quad i = 1, \dots, n \quad (11)$$

Equation (11) provides  $2n - 2$  equations that can uniquely identify the  $2n - 2$  unknown initial conditions  $\{y_1, \dots, y_{n-1}, \alpha_1, \dots, \alpha_{n-1}\}$ . Choose  $N$  equally spaced time points  $\{t_1^{(i)}, \dots, t_N^{(i)}\}$  in each interval  $[T_{i-1}, T_i]$ ,  $i = 1, \dots, n$ . Setting  $y_{\text{model}}(t) = y_m(t)$  for  $t \in \{t_1^{(i)}, \dots, t_N^{(i)}, i = 1, \dots, n\}$  gives a set of  $nN$  equations in  $3n + 1$  unknown parameters  $\{y_0, \dots, y_{n-1}, \alpha_0, \dots, \alpha_{n-1}, c_1, \dots, c_n, k\}$ , which can easily be solved by linear least squares with the equality constraints defined in Equation (11). The result determines the best fit time varying damping model of Equation (3) to the measured data.

Note that the previous integral method [13] was developed on over-damped systems and only required a single initial condition. For second order systems, the response

can be oscillatory and has two initial conditions including the derivative. Furthermore, the time-varying damping is globally constrained over the whole data interval thus requiring a different treatment of the equations compared to the reference in [12].

### C. Integral method – Constant damping parameter

A major advantage of the proposed time varying algorithm is that it allows for flexibilities in describing non-linear damping. For example, the damping values  $c_1, \dots, c_n$  in Equation (4) could be allowed to vary within bounds, or the relative difference  $|c_i - c_{i-1}|$  could be kept within a given amount based on known physical constraints. A physical law can then be derived by relating the identified damping to measurable quantities like velocity or displacement.

The simplest possible constraints to put on the damping values onto the identified damping values is the equality constraints  $c_1 = c_2 = \dots = c_n = c$ . This constraint is important as it allows a comparison of the suitability of more complex models compared to simpler models. For constant damping model, the equality constraints of Equation (11) are not required. Setting  $y_{\text{model}}(t) = y_m(t)$  for  $t \in \{t_1^{(i)}, \dots, t_N^{(i)}, i = 1, \dots, n\}$  gives a set of  $nN$  equations in 4 unknowns  $\{y_0, \alpha_0, c, k\}$ , which is solved by linear least squares to yield a best fit match of the constant damping model to the measured data.

## III. RESULTS & DISCUSSION

### A. Parameter identification of an electro-mechanical cart system

1) *Setup and Data Acquisition:* A schematic of the cart system is shown in Figure 1. The cart can move back and forward along a support rail. The cart is tethered and has two wires, one for the commanded voltage and another for feedback of the cart position which is achieved using an encoder. The origin is set at the middle of the track. The cart system is connected to a dSpace system with Control Desk [15] to allow real-time access to changing control gains, for data acquisition and viewing the signals. A proportional-integral-derivative (PID) controller is designed in Simulink which is then compiled into C code. All data is saved as a .mat file in Matlab, and includes the voltage input (V) and cart position (m) which are measured at 1kHz. The cart is powered by a 12 V DC motor.

2) *Cart modelling:* The net normalized force applied to the cart is the force from the input voltage less the damping force:

$$\ddot{y} = \beta V(t) - C\dot{y} \quad (12)$$

where  $V(t)$  is applied voltage (V),  $y$  is cart displacement (m),  $\dot{y}$  is cart velocity ( $ms^{-1}$ ),  $\ddot{y}$  is cart acceleration ( $ms^{-2}$ ), The damping coefficient  $C$  is a lumped parameter which includes armature resistance, friction of the gears and track. The parameter  $\beta$  is a normalized voltage constant ( $NV^{-1}$ ), which includes the gearing ratio and torque constant of the DC motor.

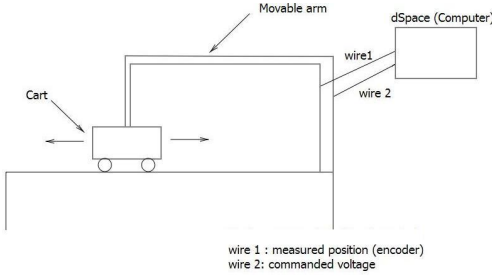


Fig. 1. Electromechanical cart system setup.

In this paper, a proportional-derivative (PD) controller is considered. The data used is obtained by setting the derivative gain  $K_d = 0$ , and the reference  $r(t) = r_0$  which is a closed loop step response. A closed loop response is used for the identification to ensure a stable oscillatory response from the cart. Note that a step response has infinitely many sinewaves, so in principle provides all the dynamics necessary for identification.

The goal of the system identification is to identify the parameters  $\beta$  and  $C$  in Equation (12) so that a wide range of control responses can be predicted for various gains  $K_p$  and  $K_d$  without requiring further experiments. For  $r(t) = r_0$ , the model of Equation (12), with PD control, is rewritten:

$$\ddot{e} + \bar{C}\dot{e} + \bar{\beta}e = 0 \quad (13)$$

$$\bar{C} = C + \beta K_d, \quad \bar{\beta} = \beta K_p \quad (14)$$

Hence, with PD control the cart system acts as a spring-mass-damper with damping  $\bar{C}$  and an analogous “stiffness” of  $\bar{\beta}$ . In terms of the displacement  $y(t)$ , Equation (13) is equivalent to:

$$\ddot{y} + (C + \beta K_d)\dot{y} + \beta K_p y = \beta K_p r_0, \quad r_0 = 0.1 \quad (15)$$

Figure 2(b) shows the measured step responses of the cart with  $K_p = 60$  and  $K_d = 0$  and with the reference displacement shown in Figure 2(a). This reference response alternates from ‘0’ position to 0.1m. The voltage input for the measured step response  $V_{in}(t)$  ranges from -2.3 V to 5.9V with a mean of 0.3V.

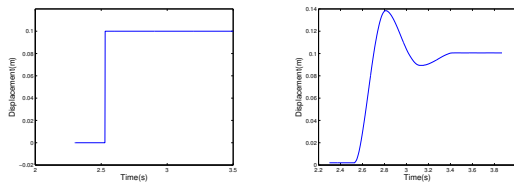


Fig. 2. (a) Reference displacement for cart system (b) Measured displacement response

3) *Constant damping model:* As an initial approximation, a constant damping model is assumed. Parameters  $\bar{C}$  and  $\bar{\beta}$  are first identified and  $C$  and  $\beta$  are calculated from:

$$C = \bar{C} - \frac{\bar{\beta}}{K_p} K_d, \quad \beta = \frac{\bar{\beta}}{K_p} \quad (16)$$

The experimental data used is the first step response of Figure 2(b). The response is transformed into the measured error response, where  $r(t) = r_0 = 0.1m$ . The starting time of  $t = 0$  is taken to be the point that the cart velocity first goes non-zero in Figure 2(b). The identified  $C$  and  $\beta$  from the constant damping model are:

$$C_{60} = 6.1520 \quad \beta_{60} = 1.8545. \quad (17)$$

where the subscript ‘60’ refers to the experimental gain  $K_p$  used to obtain the measured data. The resulting modelled response (solid) versus measured response (dots) is shown in Figure 3. The constant damping model captures the measured response closely in the first peak, but start to deviate in the second peak. This error is due to not capturing the non-linear effects such as static friction.

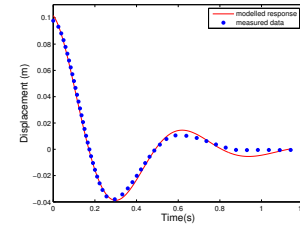


Fig. 3. Identified constant parameter modelled response (solid) versus measured error response (dotted) of cart for a step input of  $r(t) = 0.1$  m

4) *Time varying damping:* It is now assumed that the unknown damping parameter  $C$  in Equation (12) varies across time step  $\Delta t = 0.15s$ . This interval is again based on computing half the smallest zero crossing time interval  $\Delta t_{1/2}$ . This choice is arbitrary, but keeps the total number of damping values small for minimizing computation while ensuring accurate capture of non-linear effects. Applying the time varying model identification algorithm gives  $\beta = 1.9352$  and a sequence of six values for  $c(t)$  in Equation (4) and is plotted in Figure 4. Figure 4 shows a net trend of increasing damping over time. Towards the latter part after 0.5s, the damping is greater which corresponds to when the velocity of the cart starts to significantly decrease so that static friction dominates. The jumps and “noise” in the damping values are due to the fact that several sections of the data in Figure 3 are close to linear, for example, at between 0 and 0.16, and 0.32 and 0.48. To avoid the jumps, the algorithm is solved with the constraints:

$$c_1 - c_2 < \delta, \quad c_2 - c_3 < \delta, \quad \dots, \quad c_5 - c_6 < \delta \quad (18)$$

Figure 5 shows the identified damping values for the choice of  $\delta = 0.5$  in Equation (18). The value of  $\delta$  is chosen to be slightly positive to reflect the general trend of increasing damping over time as suggested by Figure 5. The similar trend is still present, and for Figure 5,  $\beta = 1.9165$ , as compared to  $\beta = 1.9352$  without constraints. This 0.9% change shows that the voltage constant is essentially unaffected by the constraints of Equation (18). The model

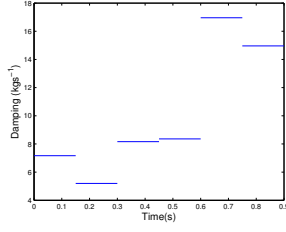


Fig. 4. Identified time varying damping  $c(t)$  as defined in Equation (4)

matches for the two constraint levels is shown in Figure 6(a). The mean absolute displacement error for each case is 0.00309 m and 0.00257 m respectively, showing that the constraints have little effect on the overall response.

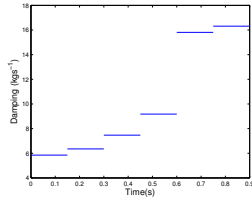


Fig. 5. Identified time varying damping  $c(t)$  as defined in Equation (4) for the choice of  $\delta = 0.5$  in Equation (18).

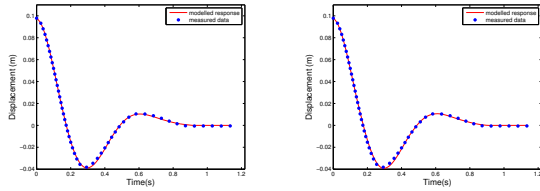


Fig. 6. (a) Model match for  $\delta = \infty$  and (b) Model match for  $\delta = 0.5$ .

5) *Damping as a function of velocity*: Each damping value in Figure 5 is defined over a constant interval of  $\Delta t = 0.15s$ . An approximate representation of the velocity during each interval is the mean velocity  $\bar{v}_i$ , which is defined:

$$\bar{v}_i = \frac{1}{\Delta t} \int_{T_{i-1}}^{T_i} v(t) dt, \quad i = 1, \dots, 6 \quad (19)$$

Plotting  $\bar{v}_i$  for each interval  $i = 1, \dots, 6$  suggests an exponential model for relating damping to velocity:

$$C(v) = \alpha_1 e^{-\alpha_2 v} + \gamma \quad (20)$$

Let  $C_m(v)$  denote the measured damping versus velocity data. Setting  $C(v_i) = C_m(v_i)$  yields the equations:

$$\alpha_1 e^{-\alpha_2 v_i} = C_m(v_i), \quad i = 1, \dots, 6 \quad (21)$$

For a given estimate of  $\gamma$ , let  $\alpha_{1,\gamma}$  and  $\alpha_{2,\gamma}$  be the linear least squares solution to Equation (21). Define:

$$F(\gamma) = \sum_{i=1}^6 (\alpha_{1,\gamma} e^{-\alpha_{2,\gamma} v_i} + \gamma - C_m(v_i))^2 \quad (22)$$

Minimizing  $F(\gamma)$  of Equation (22) by non-linear regression in Matlab gives the required parameters for the damping model.

The final non-linear model of the error response (for the case of  $\delta = 0.5$ ) in Equation (13) is defined:

$$\ddot{e} + (\alpha_1 e^{-\alpha_2 |e|} + \gamma)\dot{e} + \bar{\beta}e = 0 \quad (23)$$

$$\alpha_1 = 17.3264, \quad \alpha_2 = 13.1068, \quad \gamma = 5.9986, \quad \beta_{60} = 1.9165. \quad (24)$$

The equivalent form of Equation (23) in terms of the measured displacement is:

$$\ddot{y} + (\alpha_1 e^{-\alpha_2 |y|} + \gamma)\dot{y} + \bar{\beta}(y - r_0) = 0, \quad r_0 = 0.1 \quad (25)$$

The plots of the solution to Equation (23) and (25) are given in Figures 7(a) and 7(b) which show a close match to the data. The modelled response in Figure 6(a) captures the fast decay to zero quite closely and is significantly more accurate than the linear model of Figure 2(b).

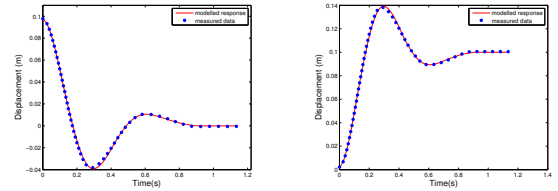


Fig. 7. (a) Identified non-linear model response (solid) of the cart from Equation (23) against measured error response (dotted) and (b) Identified non-linear model response (solid) of the cart from Equation (25) against measured cart displacement (dotted)

## B. System identification with different proportional gains

To further test the proposed algorithms, they are applied separately to step error responses of the cart with  $K_p = 80$  and  $K_p = 100$ . The identified values for the constant damping model are:

$$C_{80} = 5.4916, \quad \beta_{80} = 1.7482 \quad (26)$$

$$C_{100} = 4.5866, \quad \beta_{100} = 1.7866 \quad (27)$$

For the time varying damping model, the best fit exponential model are found for  $K_p = 80$  and  $100$  from Equations (20) - (22) as was done for  $K_p = 60$ . The non-linear damping parameters for  $K_p = 80$  and  $K_p = 100$  are:

$$\alpha_{1,80} = 22.1357, \quad \alpha_{2,80} = 18.2233, \quad \gamma_{80} = 5.6035, \quad \beta_{80} = 1.9180 \quad (28)$$

$$\alpha_{1,100} = 15.2528, \quad \alpha_{2,100} = 5.9934, \quad \gamma_{100} = 3.7990, \quad \beta_{100} = 1.9100 \quad (29)$$

Figure 8 shows the resulting exponential damping models superimposed with the damping model for  $K_p = 60$ . In addition, the  $\beta$  values are identified to be 1.9165, 1.9180, and 1.9100, for  $K_p = 60, 80$  and  $100$  respectively.

Figure 8 is an important validation as the three different sets of  $K_p$  gains 60, 80, and 100 give three very different cart responses, with voltage input ranges of  $[-2.3 \text{ V}, 5.9 \text{ V}]$ ,  $[-4.0 \text{ V}, 8.0 \text{ V}]$  and  $[-6.1 \text{ V}, 9.9 \text{ V}]$  respectively. Yet, similar damping values and virtually identical  $\beta$  values are obtained.

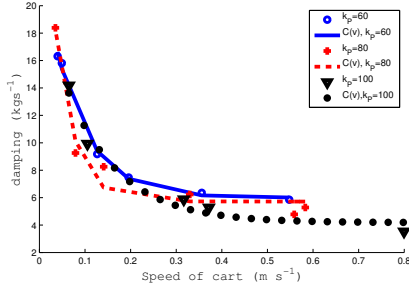


Fig. 8. Resulting exponential models for  $K_p = 80$  and  $100$  superimposed onto the identified damping model for  $K_p = 60$

For the purposes of comparison, define three different linear models  $Lm_1$ ,  $Lm_2$ ,  $Lm_3$  as follows:

$$Lm_1 \equiv \text{solution to Equation (15) with } C = C_{60} \text{ and } \beta = \beta_{60} \text{ from Equation (17) and arbitrary gains } K_p \text{ and } K_d, \quad (30)$$

$$Lm_2 \equiv \text{solution to Equation (15) with } C = C_{80} \text{ and } \beta = \beta_{80} \text{ from Equation (26) and arbitrary gains } K_p \text{ and } K_d \quad (31)$$

$$Lm_3 \equiv \text{solution to Equation (15) with } C = C_{100} \text{ and } \beta = \beta_{100} \text{ from Equation (27) and arbitrary gains } K_p \text{ and } K_d \quad (32)$$

Similarly, three non-linear models  $NLm_1$ ,  $NLm_2$  and  $NLm_3$  are defined:

$$NLm_1 \equiv \text{solution to Equation (15) with } \beta = \beta_{60} \text{ and } C = C(v) \text{ from Equation (20), with } \alpha_1 = \alpha_{1,60}, \alpha_2 = \alpha_{2,60}, \gamma = \gamma_{60} \text{ from Equation (24)} \quad (33)$$

$$NLm_2 \equiv \text{solution to Equation (15) with } \beta = \beta_{80} \text{ and } C = C(v) \text{ from Equation (20), with } \alpha_1 = \alpha_{1,80}, \alpha_2 = \alpha_{2,80}, \gamma = \gamma_{80} \text{ from Equation (28)} \quad (34)$$

$$NLm_3 \equiv \text{solution to Equation (15) with } \beta = \beta_{100} \text{ and } C = C(v) \text{ from Equation (20), with } \alpha_1 = \alpha_{1,100}, \alpha_2 = \alpha_{2,100}, \gamma = \gamma_{100} \text{ from Equation (29)} \quad (35)$$

The models of  $Lm_1$ ,  $Lm_2$ ,  $Lm_3$  in Equations (30) - (32) and  $NLm_1$ ,  $NLm_2$  and  $NLm_3$  in Equations (33) - (35) can be used to test any sets of gains  $K_p$  and  $K_d$  in Equation (15).

Figures 9(a) and 9(b) show the resulting model matches to the experimental data for the non-linear models  $NLm_2$  and  $NLm_3$  and the constant damping models  $Lm_2$  and  $Lm_3$ . The mean absolute error in the displacement in Figure 9(a) are 0.0071 m for the linear model  $Lm_2$  and 0.001 m for the non-linear model  $NLm_2$ . For Figure 9(b), the mean errors are 0.0074 m for the linear model  $Lm_3$  and 0.0017 m for the non-linear model  $NLm_3$ . Thus, in both cases the fitting error is reduced by a factor of 7.

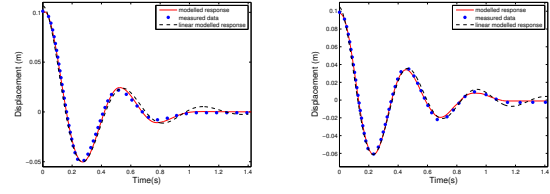


Fig. 9. (a) Model matches to experimental data for  $K_p = 80$  and (b) Model matches to experimental data for  $K_p = 100$

### C. PD control response predictions

A further proof-of-concept of the characterization method is to test the ability of the linear and non-linear identified response models to predict PD control responses to a reference step input  $r(t) = 0.1m$  for a number of different gains.

Figures 10(a) and 10(b) show that the non-linear damping model  $NLm_1$  significantly outperforms the constant damping model  $Lm_1$ . Table I give the percentage error of the mean absolute value between the measured and model responses for a number of PD control experiments using the six models  $Lm_1$ ,  $Lm_2$ ,  $Lm_3$ ,  $NLm_1$ ,  $NLm_2$  and  $NLm_3$  from Equations (30) - (35). On average, the non-linear model  $NLm_1$  has an error of 3.7% which is much smaller than the linear model  $Lm_1$  prediction error of 9.3%. Similarly, the non-linear models  $NLm_2$  and  $NLm_3$  have average errors of 3.9% and 4.3% which are much smaller than the corresponding errors for the linear models  $Lm_2$  and  $Lm_3$  which are 10.6% and 10.6%. Hence, for the non-linear case, equally good models are obtained regardless of specific experimental data used to identify the parameters. This result further validates the time varying damping method presented in this paper.

PD response		Constant damping			Non-linear model		
$K_p$	$K_d$	$Lm_1$	$Lm_2$	$Lm_3$	$NLm_1$	$NLm_2$	$NLm_3$
60	0	7.0	18.96	18.73	1.0	3.84	5.63
60	5	8.24	9.20	10.10	3.0	4.80	5.87
80	0	11.08	7.1	12.04	4.70	1.10	6.12
80	5	5.95	4.65	3.95	3.76	3.39	3.53
80	10	14.3	15.05	15.97	3.21	3.01	3.78
100	0	14.71	17.5	7.4	6.50	6.93	1.70
100	5	3.25	3.97	4.72	2.81	3.10	3.55
100	10	9.70	8.93	11.50	4.60	5.20	4.00
Average error		9.3	10.6	10.6	3.7	3.9	4.3

TABLE I  
PERCENTAGE ERROR COMPARISON OF THE LINEAR AND NON-LINEAR MODELS FOR EACH SET OF PD GAINS USING THREE DIFFERENT MODEL CHARACTERIZING SETS.

### D. Controller design

To further prove the importance of the non-linear model in control design, a simple PD controller is constructed based on the following specifications:

Given  $K_p = 100$ , minimize  $K_d$  such that settling time (1%)  $\leq 0.5s$  (36)

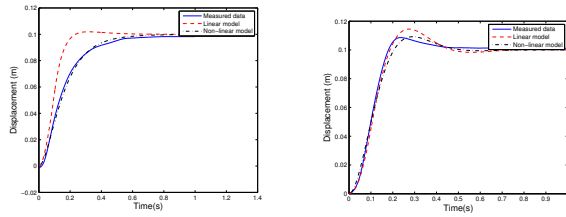


Fig. 10. (a) Predicted responses for the case of  $K_p = 80$ ,  $K_d = 10$  using  $Lm_2$  of Equation (31) and  $NLm_2$  of Equation (34) and (b) Predicted responses for the case of  $K_p = 100$ ,  $K_d = 5$  using  $Lm_3$  and  $NLm_3$ .

These specifications in Equation (36) are met with both the linear model  $Lm_3$  of Equation (32) and the non-linear model  $NLm_3$  of Equation (35).

For the linear model the  $K_d$  gain was computed to be 7.35 and for the non-linear model, the  $K_d$  gain was 3.55. Hence, for this example, the derivative gain for the linear approach was more than twice the non-linear. In practice, a higher derivative gain would require significantly more smoothing on the data to avoid the derivative control over-responding to noise, which would in turn create more time lag further affecting control. In other words, the smaller the  $K_d$  gain designed to meet the specifications, the more effective and easier to implement, the controller will be. Hence these results demonstrate the importance of characterizing the non-linear dynamics of the system.

#### IV. CONCLUSIONS

A simplified modelling approach and integral based parameter identification method was used to identify and analyze a number of non-linear mechanical cart system responses. Two cases of constant and time-varying parameter models of damping were considered. For the time-varying damping model, coefficients were identified across time intervals equally spaced across the data. The damping values were related to the absolute value of velocity by a decaying exponential function, revealing increased friction or “stiction” that occurs at small velocities and includes the dynamics of gear backlash. This new model was then applied to PD control responses with a step input over a range of gains. For each of these predictions, only one data set was used to identify the model. The model predicted a smaller mean absolute error cart displacement of a PD controlled step response for eight sets of PD gains. Hence the model and method proved very accurate for a wide range of dynamics and input voltages for this electromechanical cart system.

There are many quite complex models in the literature for capturing this behaviour of the static friction, gear backlash and other non-linearities in electro-mechanical systems. These typically make strong initial assumptions on the model then match this model to the data. The approach in this paper is to initially have no assumption on the precise model for friction but to let the damping vary over time in a relatively simple model, then correlate the resulting damping values to measured quantities like velocity or displacement. The

resulting model is a lumped parameter model that captures the observed non-linear behaviour. Hence, the philosophy is to start with simplified models and add complexity as required to better predict experimental responses.

In addition, a simple PD controller was constructed based on a set of specifications, including overshoot and settling times. Overall it demonstrates the concept of using a non-linear model to significantly minimize the number of experiments required in PD tuning as compared to a standard linear modeling approach. This differs from the usual approach, which is to let the complex controller itself deal with the modeling error. Hence this research puts the emphasis on developing a systematic approach that can build complex non-linear models from simplified models and give greater confidence in the performance of control methods.

Finally, the identification algorithm was shown to be up to 7800 times faster than standard non-linear regression showing that it has very minimal computation requirements and is thus a useful tool for modelling second order systems.

#### REFERENCES

- [1] Chopra K. *Dynamics of Structures: Theory and Application to Earthquake engineering* (3rd edn). Pearson Prentice Hall, Upper Saddle River, 2007, 687-795.
- [2] Ge, S.S, Huang, L and Lee, T.H, Position Control of Chained Multiple Mass-Spring-Damper Systems Adaptive Output Feedback Control Approaches, *Int. J. Contr. Autom. and Sys.*, 2004, 2(2): 144-155.
- [3] Velotsos, A.S and Ventura, C.E. Modal Analysis of Non-classically damped linear systems. *Jour. Earthq. Engr. and Str. Dyn.*, 1986. 14: 217-243.
- [4] Kumaresan, R and Tufts, D. 1982. Estimating the parameters of exponentially damped sinusoids and pole-zero modeling in noise. *IEEE. Trans. Acoust. Speech, Signal Process.*, ASSP-30: 833-840.
- [5] McGowan, R. S, Smith, C. L, Browman, C. P and Kay, B.A. Methods for Least-squares Parameter Identification for Articulatory Movement and the Program PARFIT. *Haskin Lab Status Report on Speech Research*, SR-101/102, 1990: 220-230.
- [6] Kay, S and Saha, S. Mean Likelihood Frequency Estimation. *IEEE Trans. Sig. Proc.*, 2000; 48(7):1937-1946.
- [7] Wolm, P, Chen, X. Q, Chase, J. G, Pettigrew, W and Hann, C. E. Analysis of a PM DC motor model for application in feedback design for electric-powered mobility vehicles. *Int. J. Comp. App. Tech.*, 2010; 39(1-3):116-122.
- [8] Spencer, B. F Jr, Dyke, S. J., Sain, M. K., Carlson, J. D. Phenomenological model of a magnetorheological damper, *J. Eng. Mech.*, 1997; 123(3): 230-238.
- [9] Wen, Y. K. Method of Random Vibration of Hysteretic Systems, *ASME J. Eng. Mech. Div.*, 1976; 2(EM2):249-263.
- [10] Dion, J-L., Le Moyne, S., Chevallier, G., Sebbah, H. Gear impacts and idle gear noise: Experimental study and non-linear dynamic model, *J. Mech. Syst. Sig. Proc.*, 2009; 23(8):2608-2628.
- [11] lu, V.P and Cheung, Y. K. Non-linear vibration analysis of multilayer beams by incremental finite elements, Part II: Damping and forced vibrations. *J. Sound. Vib.*, 1982; 100(3):373-382.
- [12] Hann, C. E., Chase, J. G. Lin, J., Lotz, T., Doran, C. V. and Shaw, G. M. Integral-Based Parameter Identification For Long-Term Dynamic Verification Of A Glucose-Insulin System Model. *Comput. Methods. Progr. Biomed.*, 2005; 77:259-270.
- [13] Starfinger, C. Hann, C. E., Chase, J. G., Desai, T., Ghuysen, A. and G. M. Shaw. Model-based cardiac diagnosis of Pulmonary Embolism. *Comput. Methods. Programs. Biomed.*, 2007; 87(1):pp. 46-60.
- [14] Hann, C. E. Snowdon, M. H. Rao, A. A. Winn, O. Wongvanich, N. and Chen, X. Q. Minimal Modelling Approach to Describe Turbulent Rocket Roll Dynamics in a Vertical Wind Tunnel. *Proc. of IMechE. part G, J. Aero. Eng.*, 2011.
- [15] dSPACE GmbH DS1103 PPC Controller Board, Catalogue. *dSpace Catalogue*, 2011; 290-295.
- [16] Gopal, M. *Control Systems: Principles and Design*, Tata McGraw-Hill, New Delhi, 2008, 672-673.